

# Localization and stretching of polymer chains at the junction of two surfaces

Cite as: J. Chem. Phys. **140**, 204909 (2014); <https://doi.org/10.1063/1.4878499>

Submitted: 01 December 2013 . Accepted: 06 May 2014 . Published Online: 27 May 2014

Tarak K. Patra, and Jayant K. Singh



View Online



Export Citation



CrossMark

## ARTICLES YOU MAY BE INTERESTED IN

[Coarse-grain molecular dynamics simulations of nanoparticle-polymer melt: Dispersion vs. agglomeration](#)

The Journal of Chemical Physics **138**, 144901 (2013); <https://doi.org/10.1063/1.4799265>

[Thermal conductivity of thermoelectric material  \$\beta\$ -Cu<sub>2</sub>Se: Implications on phonon thermal transport](#)

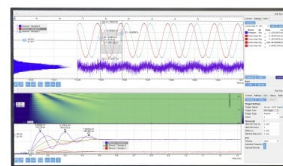
Applied Physics Letters **111**, 163903 (2017); <https://doi.org/10.1063/1.4999405>

[Melting transition of Lennard-Jones fluid in cylindrical pores](#)

The Journal of Chemical Physics **140**, 204703 (2014); <https://doi.org/10.1063/1.4876077>

Challenge us.

What are your needs for  
periodic signal detection?



Zurich  
Instruments



# Localization and stretching of polymer chains at the junction of two surfaces

Tarak K. Patra and Jayant K. Singh<sup>a)</sup>

Department of Chemical Engineering, Indian Institute of Technology Kanpur, Kanpur 208016, India

(Received 1 December 2013; accepted 6 May 2014; published online 27 May 2014)

We present a molecular dynamics study on the stretching of a linear polymer chain that is adsorbed at the junction of two intersecting flat surfaces of varying alignments. We observe a transition from a two-dimensional to one-dimensional (1D) structure of the adsorbed polymer when the alignment, i.e., the angle between the two surfaces that form a groove,  $\theta$ , is below  $135^\circ$ . We show that the radius of gyration of the polymer chain  $R_g$  scales as  $R_g \sim N^{3/4}$  with the degree of polymerization  $N$  for  $\theta = 180^\circ$  (planar substrate), and the scaling changes to  $R_g \sim N^{1.0}$  for  $\theta < 135^\circ$  in good solvents. At the crossover point,  $\theta = 135^\circ$ , the exponent becomes 1.15. The 1D stretching of the polymer chain is found to be 84% of its contour length for  $\theta \leq 90^\circ$ . The center of mass diffusion coefficient  $D$  decreases sharply with  $\theta$ . However, the diffusion coefficient scales with  $N$  as  $D \sim N^{-1}$ , and is independent of  $\theta$ . The relaxation time  $\tau$ , for the diffusive motion, scales as  $\tau \sim N^{2.5}$  for  $\theta = 180^\circ$  (planar substrate), which changes to  $\tau \sim N^{3.0}$  for  $\theta \leq 90^\circ$ . At the crossover point, the exponent is 3.4, which is slightly higher than the 1D value of 3.0. Further, a signature of reptation-like dynamics of the polymer chain is observed at the junction for  $\theta \leq 90^\circ$  due to its strong 1D localization and stretching. © 2014 AIP Publishing LLC. [<http://dx.doi.org/10.1063/1.4878499>]

## I. INTRODUCTION

Polymer-surface interfaces are researched with great interest owing to their importance in micro/nanofluidic devices, coating, adhesion, wetting, single molecule characterization, DNA sequencing, protein structure analysis, and several biophysical processes.<sup>1,2</sup> A polymer chain at a solid interface reduces its conformational entropy due to the presence of an impenetrable surface and gains enthalpy due to the bonding with the surface. This causes profound structural and dynamical changes to the polymer with respect to its bulk state.<sup>3</sup> However, solid surfaces can be designed to control the structure and dynamics of macromolecules. For example, a nano-patterned surface,<sup>4</sup> an entropic trap,<sup>5</sup> a ratchet slit,<sup>6</sup> and an orthogonal surface<sup>7</sup> enhance the fractionation of DNA and other macromolecules compared to a smooth surface. A polymer chain in such constrained geometries experiences anomalous diffusion, entropic trapping, loop-train conformation, adsorption-desorption, and reptation, etc.<sup>5,8-10</sup> Further, a recent experiment shows that DNA molecules can be remarkably stretched along a particular direction on a lipid membrane supported on a grooved, one-dimensional (1D) periodic micro-structured surface.<sup>11</sup> On the other hand, two-dimensional (2D) conformation of DNA is observed on a lipid membrane supported on a flat surface.<sup>10,12</sup> Such an unexpected impact of the grooved or archetypical substrate is noteworthy and can be used to unfold DNA molecules in an open environment, giving insight into previously inaccessible states when in their natural three-dimensional (3D) environment. The unfolding of macromolecules plays an important

role for their characterization, sequencing, and understanding their intermolecular interactions.<sup>13</sup> DNA molecules are also found to stretch in an open-channel, and approach their full contour length as the width of the channel decreases.<sup>14</sup> Further, efficient electrophoresis of DNA molecules across an orthogonal surface of a microchannel has been observed.<sup>7</sup> The structure of a DNA molecule on such narrow geometries, which are essentially a junction of two flat surfaces, appears to be 1D. The aim of the present work is to understand the structure and dynamics of a polymer at a junction where two flat surfaces intersect and form a groove. Using molecular dynamics (MD) simulations of a generic model system, we study the change in the radius of gyration ( $R_g$ ), diffusion coefficient ( $D$ ), and the relaxation time ( $\tau$ ) of polymer chains at the junction when the angle between the two surfaces changes. We further analyze the stretching of a linear polymer chain under such confinements.

The scaling relations between  $R_g$ ,  $D$ , and  $\tau$  of a polymer chain with its size at the junction of two surfaces are of added interest. Under constrained geometries such as cylindrical, spherical, parabolic, and slit-like pore,  $R_g$ ,  $D$ , and  $\tau$  of a polymer chain follow power law scaling with its length ( $N$ ) and width of the confinement.<sup>15,16</sup> However, the scaling relations at the junction of two surfaces are not well understood. As expected for a self-avoiding walk,  $R_g \sim N^\gamma$ , where the exponent is related to the dimension of the polymer  $d$  as  $\gamma = 3/(d + 2)$  for good solvent conditions.<sup>17</sup> Therefore,  $R_g$  of an adsorbed polymer chain on a flat surface scales as  $R_g \sim N^{3/4}$ , as its conformation becomes 2D on the surface.<sup>18</sup> Similarly, the scaling relation for the 1D structure is  $R_g \sim N^{1.0}$ .<sup>19</sup> However, it is not clear how the scaling relations change as the conformation of a polymer is forced from 2D to 1D, such as the case of the present study.

<sup>a)</sup> Author to whom correspondence should be addressed. Electronic mail: jayantks@iitk.ac.in

Further, the geometric constraints imposed on a polymer molecule, induce significant changes in its dynamics.<sup>2</sup> The surface diffusion and relaxation are influenced by the topological details of surfaces.<sup>9,18,20,21</sup> The diffusion coefficient on a flat substrate is found to scale as  $D \sim N^{-1.0}$ ,<sup>18,22</sup> while on a corrugated surface, it is found to scale as  $D \sim N^{-1.5}$ .<sup>18</sup> In spite of the strong diffusion scaling on the corrugated surface, the authors of that study did not observe any reptation behavior. On the contrary, polyethylene glycol (PEG) adsorbed from an aqueous solution onto a monolayer of self-assembled octadecyltriethoxysilane coated onto a fused silica surface is found to reptate with  $D \sim N^{-1.5}$ .<sup>20,23</sup> The reptation of polymers in 2D is also observed with  $D \sim N^{-1.5}$  when obstacles are present in the medium.<sup>24</sup> In Rouse dynamics, the relaxation time scales as  $\tau \sim N^{1+2\gamma}$ .<sup>25,26</sup> Because  $\tau \sim R_g^2/D$ , the scaling  $D \sim N^{-1.0}$  is expected for the Rouse dynamics. Therefore, the unexpected scaling is argued to be caused by the roughness of surfaces.<sup>2,23</sup> Similarly, a polymer chain inside a cylinder stretches along the axis of the cylinder, and diffuses axially (1D) with  $D \sim N^{-1.0}$  and  $D \sim N^{-1.5}$  for smooth and corrugated surfaces, respectively.<sup>27</sup> This common observation strongly suggests that imposed topological constraints affect the dynamical scaling of a polymer, irrespective of its dimensionality. Here, we investigate the effects of topological constraints on scaling relations of a polymer chain as it transitions from 2D to 1D structure at the junction of two flat surfaces. To model such a junction or grooved substrate, we take two flat surfaces and place them at different alignments. The angle between the two surfaces,  $\theta$ , is considered as the measure of alignment. The scaling relations are derived for four alignments, namely,  $45^\circ$ ,  $90^\circ$ ,  $135^\circ$ , and  $180^\circ$  (planar substrate).

The aim of the present study is to understand the usefulness of angular confinement in stretching a macromolecule, and derive scaling relations for its  $R_g$ ,  $D$ , and  $\tau$  with size, at the junction of two surfaces. The rest of this paper is organized as follows. The model of the polymer chain and surface, along with the simulation method used, is described in Sec. II. In Sec. III, we present the results and discussion, followed by conclusions in Sec. IV.

## II. MODEL AND METHODS

We use a coarse-grained model that has been successful in reproducing generic features of many experimental findings.<sup>2,18,28</sup> In this generic model, a polymer is represented by a chain of beads that interact via the Lennard-Jones (LJ) potential,

$$V(r) = 4\epsilon \left[ \left( \frac{r}{\sigma} \right)^{12} - \left( \frac{r}{\sigma} \right)^6 \right] - V(r_c), \quad (1)$$

where  $\epsilon$  and  $\sigma$  are the characteristic energy and length scales, respectively. The results are presented in terms of  $\epsilon$ ,  $\sigma$ , and  $m$ , where  $m$  is the mass of a bead. The cut-off distances,  $r_c$ , for good and poor solvents, are  $2^{1/6}\sigma$  and  $2 \times 2^{1/6}\sigma$ , respectively. In addition, any two adjacent beads in a polymer chain are connected by a finitely extensible non-linear elastic (FENE)

potential,<sup>29</sup>

$$V^{FENE} = \begin{cases} -\frac{1}{2}kR_0^2 \ln \left[ 1 - \left( \frac{r}{R_0} \right)^2 \right] & \text{for } r < R_0 \\ \infty & \text{for } r \geq R_0 \end{cases}. \quad (2)$$

Here,  $k = 30\epsilon\sigma^{-2}$  and  $R_0 = 1.5\sigma$ . The choice of these parameters prevents the crossing of any bonds in a chain. The surface is modeled as the (111) plane of an fcc lattice. Surface atoms are placed at lattice sites with neighbor distance of  $1\sigma$ . As mentioned earlier, each confined substrate consists of two flat surfaces whose geometries are square, and the linear dimension is at least twice the length of a fully stretched polymer chain. An attractive surface-polymer interaction is chosen to model strong adsorption of the polymer chains. Polymer beads and surface atoms interact with the same potential as that of polymer beads interacting with each other in poor solvent conditions. The surface atoms have been frozen to ensure a static free energy barrier.<sup>27</sup>

Equations of motion are integrated using the velocity-Verlet algorithm<sup>30</sup> with a time step of  $0.005\tau_0$ , where  $\tau_0 = \sigma\sqrt{m/\epsilon}$  is the unit of time. All the simulations are performed at a temperature  $T = 1.0\epsilon/k_B$ , imposed using a Langevin thermostat, with coupling constant  $\gamma = 0.1\tau_0^{-1}$ .<sup>16</sup> Here,  $k_B$  is the Boltzmann constant. The initial configurations are equilibrated for  $10^8$  steps, followed by a production cycle of  $10^8$  steps. We ensure that the polymer chain has moved a distance several times of its own size during equilibration. All the simulations are carried out using the LAMMPS software package.<sup>31</sup>

## III. RESULTS AND DISCUSSION

In Fig. 1, we show the conformations of a chain of 100 beads at the junction of two surfaces with different alignments. When the angle between the two surfaces is  $\theta = 180^\circ$ , i.e., a planar substrate, the conformation of an adsorbed chain is 2D. However, for  $\theta < 180^\circ$ , it tends to localize along the line of intersection between the two surfaces. The size of the polymer chain in different directions can be quantified by its radius of gyration:

$$\langle R_g^2 \rangle = \frac{1}{N} \sum_{i=1}^N \langle (R_i - R_{CM})^2 \rangle. \quad (3)$$

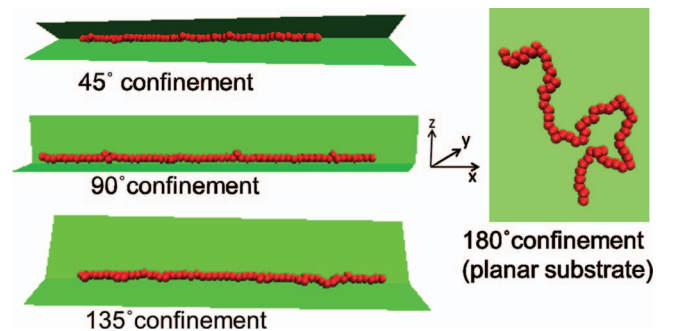


FIG. 1. The conformations of a chain of 100 beads at the junction of two intersecting flat surfaces of varying alignments in good solvents. Substrates are shown smooth for clarity.

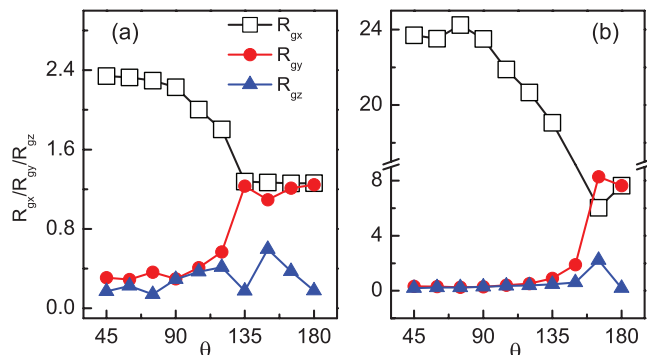


FIG. 2. The three components of the radius of gyration  $R_g$  of a polymer as a function of alignment,  $\theta$ . Panels (a) and (b) correspond to  $N = 10$  and  $N = 100$ , respectively, for good solvent conditions. Error bars are smaller than symbol sizes. Symbols are calculated values, and lines are to guide eyes.

Here,  $R_{CM}$  is the position co-ordinate of the center of mass of a chain of  $N$  beads, and  $R_i$  is the position co-ordinate of the  $i$ th bead. Figs. 2(a) and 2(b) represent the three components of  $R_g$ , i.e.,  $R_{gx}$ ,  $R_{gy}$ , and  $R_{gz}$ , for  $N = 10$  and  $N = 100$ , respectively, for good solvent conditions. We use the Cartesian co-ordinate system with  $x$ -axis along the line of intersection of the two surfaces. The other two mutually orthogonal axes, i.e.,  $y$ - and  $z$ -axis, are perpendicular to the  $x$ -axis, as shown in Fig. 1. At  $\theta = 180^\circ$ ,  $R_{gx}$  and  $R_{gy}$  are of equal magnitude and remain almost unchanged until  $\theta = 135^\circ$ , for the case of  $N = 10$ , as shown in Fig. 2(a). However,  $R_{gy}$  diminishes as  $\theta$  decreases further and the only significant component is  $R_{gx}$  for  $\theta < 135^\circ$ . This is clearly evident for  $\theta = 90^\circ$  and  $\theta = 45^\circ$ , where  $R_{gy}$  and  $R_{gz}$  become smaller than  $1\sigma$ . Therefore, the radius of gyration of a polymer chain along the line of intersection,  $R_{gx}$ , is significantly higher than that in other directions, leading to its 1D conformation. This indicates a single file motion of the polymer. Furthermore,  $R_{gx}$  is significantly higher for  $\theta \leq 90^\circ$  compared to that seen for  $\theta = 180^\circ$ . This implies a significant stretching of the polymer chain along the  $x$ -axis, as the angle between the two surfaces decreases. For  $N = 100$ , as shown in Fig. 2(b), the  $R_{gx}$  and  $R_{gy}$  are of equal magnitude for  $\theta = 180^\circ$ , as expected for a planar substrate. However,  $R_{gy}$  and  $R_{gz}$  become insignificant in comparison to  $R_{gx}$  at  $\theta = 150^\circ$  and  $R_{gx}$  is the only significant component when  $\theta \leq 150^\circ$ . Thus, a localization transition takes place at  $\theta = 150^\circ$ : above this, the polymer chain retains a 2D conformation, while below this it is trapped within the groove of the substrate in a 1D conformation along the  $x$ -axis. We find, for example,  $R_{gx} = 7.64 \pm 0.03$  for  $\theta = 180^\circ$ , and  $R_{gx} = 23.66 \pm 0.07$  for  $\theta = 45^\circ$ , in the case of a 100 bead chain. This is more than a 100% increase in size of the polymer chain in such a narrow confinement. Because the significant component of the radius of gyration of a polymer chain is  $R_{gx}$  for  $\theta \leq 135^\circ$ , we only consider  $R_{gx}$  for further investigation. Similarly,  $R_{gx}$  and  $R_{gy}$  are the significant components of the radius of gyration of a polymer for  $\theta = 180^\circ$ , hence we consider  $R_{g\parallel} = \sqrt{R_{gx}^2 + R_{gy}^2}$  for further analysis in the planer substrate case. To this end, we drop the suffixes of  $R_g$ , which represent directions.

The strong localization of a polymer chain at the junction can be realized by its strong adsorption energy as shown

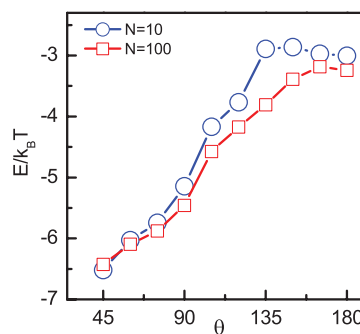


FIG. 3. The binding energy of a chain per bead on a substrate as a function of alignment for good solvent conditions. The symbols circle and square represent values for  $N = 10$  and  $N = 100$ , respectively. Lines serve as a guide to eyes. Error bars are smaller than symbol sizes.

in Fig. 3. Here, the adsorption energy is defined as the pair-interaction energy between a substrate and a polymer chain, which is shown for two cases:  $N = 10$  and  $N = 100$ . It represents the adsorption energy per bead,  $E$ , as a function of  $\theta$  for good solvent conditions.  $E$  is lowest at  $\theta = 45^\circ$ . It increases as  $\theta$  increases, and plateaus at  $\theta = 135^\circ$  for  $N = 10$ . However for  $N = 100$ ,  $E$  plateaus at  $\theta = 175^\circ$ .  $E$  is slightly higher for  $N = 10$  than that for  $N = 100$  when  $\theta \geq 90^\circ$  and, as is evident from the figure, the difference between  $E$  for  $N = 10$  and  $N = 100$  is maximum at  $\theta \sim 135^\circ$ .

Next, we look at the scaling relation of  $R_g$  with  $N$ , on the substrates. Figs. 4(a) and 4(b) represent  $R_g$  as a function of  $N$  for good and poor solvent conditions, respectively, for different alignments. At  $\theta = 180^\circ$ , we find  $R_g \sim N^{0.75}$ , but stronger scaling is observed for  $\theta < 180^\circ$ , as shown in Fig. 4(a), for good solvent conditions. For  $\theta = 90^\circ$  and  $\theta = 45^\circ$ , the exponent becomes 1.0. At the crossover point,  $\theta = 135^\circ$ , the exponent increases to 1.15. The higher exponent indicates that structural differences between two polymer chains of different lengths are highest at  $\theta = 135^\circ$ . This is in agreement with the adsorption energy difference between the chains, which displays a maximum at  $\theta = 135^\circ$ , as shown in Fig. 3. For poor solvent conditions (Fig. 4(b)), a weaker

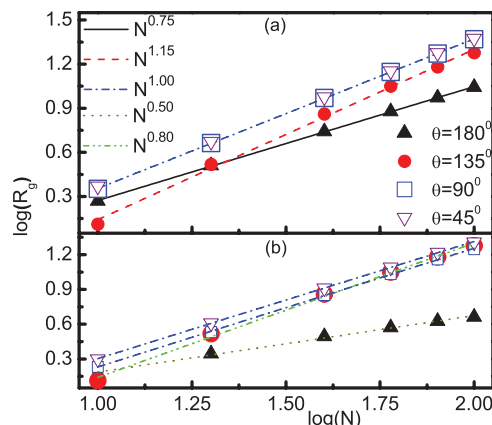


FIG. 4. The radius of gyration  $R_g$  of a polymer chain as a function of its length  $N$ . For  $180^\circ$  alignment, i.e., flat substrate,  $R_g$  is in-plane radius of gyration, and all other cases,  $R_g$  is axial radius of gyration along  $x$ -axis. Panels (a) and (b) represent data for good and poor solvent conditions, respectively. Error bars are smaller than symbol sizes.

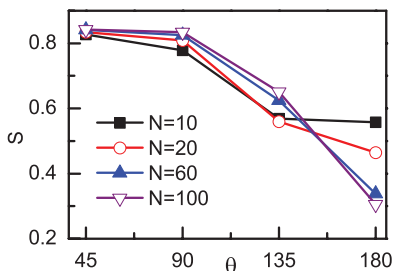


FIG. 5. The stretching of a polymer chain  $S$ , which is the ratio of its end-to-end distance to its contour length, is shown as a function of the alignment  $\theta$ . Error bars are smaller than symbol sizes. Lines are to guide eyes.

scaling is observed, with exponents 0.5 for  $\theta = 180^\circ$  and 0.8 for  $\theta = 135^\circ$ . With a further decrease in  $\theta$ , however, the exponent becomes 1.0, similar to that for good solvent conditions. This indicates the dominance of a groove-like substrate, when  $\theta \leq 90^\circ$ , on the conformation of a polymer chain, which remains uninfluenced by solvent conditions. The stretching  $S$  of a polymer chain in such confinements can be measured as

$$S = \frac{X}{L}. \quad (4)$$

Here,  $X$  and  $L$  are the end-to-end distance and contour length of a polymer chain, respectively.<sup>14</sup> Fig. 5 shows stretching as a function of alignment for four chain lengths in good solvents. Stretching is lowest at  $\theta = 180^\circ$ , i.e., on a planer substrate. Stretching increases as alignments decrease, and plateaus at  $\theta = 90^\circ$ , beyond which stretching is insignificant. A maximum of around 84% stretching is observed at  $\theta = 90^\circ$  and  $45^\circ$ .

We now focus on the diffusion of a polymer chain at the junction of the two surfaces. The diffusion coefficient of the center of mass of a polymer chain is calculated from the mean square displacement (MSD) curve,

$$g(t) = \langle [R_{CM}(t) - R_{CM}(0)]^2 \rangle. \quad (5)$$

The diffusion coefficient  $D$  is related to  $g(t)$ , showing a linear dependence with time as  $2dD = \lim_{t \rightarrow \infty} dg(t)/dt$ , where the dimensionality  $d = 2$  for  $\theta = 180^\circ$ , and  $d = 1$  for all other cases. For all chain lengths,  $D$  is calculated in the diffusive regime of  $g(t)$ , similar to our recent work.<sup>32</sup> We plot  $\log(D)$  vs.  $\log(N)$  for all the cases, in Figs. 6(a) and 6(b), for good and poor solvent conditions, respectively. As  $\theta$  decreases from  $180^\circ$ , the diffusion coefficient decreases. The dynamics is significant in the  $x$ - and  $y$ -directions for  $\theta = 180^\circ$ . However, it is only significant in the  $x$ -direction for  $\theta \leq 135^\circ$ . Hence, we calculate 2D diffusion coefficients for  $\theta = 180^\circ$ , and 1D diffusion coefficients for all other cases. The lowest diffusion is seen for the case of  $\theta = 45^\circ$ , where maximum stretching is observed. In all the cases, the diffusion coefficient scales as  $D \sim N^{-1}$ , except for  $\theta = 135^\circ$ , in poor solvents, where the exponent is slightly higher at 1.11. Our findings on the planer substrate are in agreement with that estimated from previous experiments<sup>10</sup> and simulations.<sup>18</sup> The scaling relation for the 1D structures is similar to that inside a nanotube.<sup>27</sup> In spite of a weak diffusion scaling, we see a caterpillar-like motion of the chain for  $\theta \leq 90^\circ$ , along the  $x$ -axis.

As the degree of confinement increases, we observe a significant change in the structure of a polymer chain, cou-

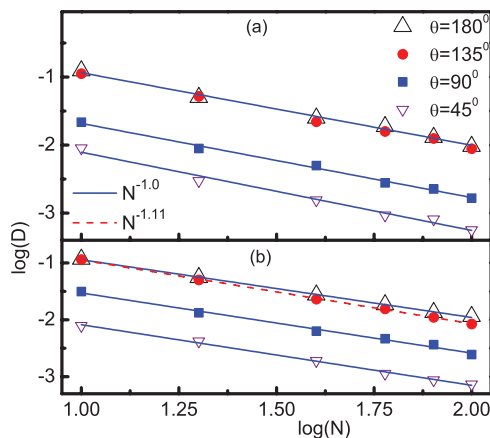


FIG. 6. The diffusion coefficient of a polymer chain  $D$  as a function of its length  $N$ . For  $180^\circ$  alignment, i.e., flat substrate,  $D$  corresponds to in-plane (2D) diffusion, and for all other cases, it is 1D along  $x$ -axis. Panels (a) and (b) represent data for good and poor solvent conditions, respectively. Error bars are smaller than symbol sizes.

pled with extremely slow dynamics. It is, therefore, important to investigate the structural relaxation of polymers under such topologically strong constrains. We estimate the relaxation time of the diffusive motion,  $\tau$ , by solving

$$g(t = \tau) = R_g^2. \quad (6)$$

This equation expresses  $\tau$  to be the time required for a chain to move a distance of the order of its own size.<sup>26,33</sup> As was done with  $D$  above, we calculate  $\tau$  in 2D for  $\theta = 180^\circ$ , and 1D for all other cases.  $\tau$  as a function of  $N$  is shown in Figs. 7(a) and 7(b), for good and poor solvent conditions, respectively. The relaxation time increases as the alignment decreases from  $\theta = 180^\circ$ , which is in agreement with slower diffusion, noted earlier. We obtain the scaling relation  $\tau \sim N^{2.5}$  on the planer substrate, i.e.,  $\theta = 180^\circ$  for good solvent conditions as shown in Fig. 7(a). The exponent is 3.0 for  $\theta \leq 135^\circ$ . For poor

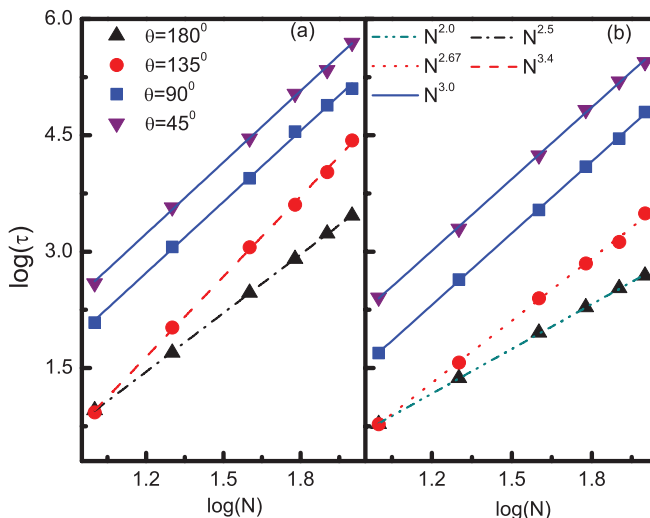


FIG. 7. The longest relaxation time  $\tau$  of a polymer chain as a function of its length  $N$ . For  $180^\circ$  alignment, i.e., flat substrate,  $\tau$  corresponds to 2D, and for all other cases, it corresponds to 1D relaxation along  $x$ -axis. Panels (a) and (b) represent data for good and poor solvent conditions, respectively. Error bars are smaller than symbol sizes.

solvent conditions, as shown in Fig. 7(b), the exponent is 2.0 for a planer substrate, and increases as the degree of confinement increases. It becomes 2.6 for  $\theta = 135^\circ$ , and goes to 3.0 for  $\theta \leq 90^\circ$ . For  $\theta \leq 90^\circ$ , the exponent is independent of solvent conditions.

#### IV. CONCLUSIONS

We presented a molecular dynamics study on the structure and dynamics of polymers at the intersection of two flat surfaces, forming a groove-like substrate. In particular, we demonstrated the localization, stretching, and crossover dynamics of a polymer chain at the junction when the angle between the two surfaces is below a critical value. The polymer chain is trapped energetically along the line of intersection of the two surfaces. It is also stretched significantly along the line of intersection of the two surfaces. The stretching increases as the angle between the two surfaces  $\theta$  decreases, taking a maximum value of around 84% of its contour length when  $\theta = 90^\circ$ , i.e., when it is an orthogonal substrate. The amount of stretching remains almost unchanged as  $\theta$  further decreases. The stretching is of the same order as that of DNA inside an open channel.<sup>14</sup> The 1D radius of gyration of a flexible polymer chain scales linearly with its length when  $\theta \leq 135^\circ$  for good solvent conditions, similar to that inside a nanotube.<sup>27</sup>

Dynamical properties of the polymer chain on the substrates are also studied. The center of mass diffusion coefficient decreases as  $\theta$  decreases. However, the diffusion coefficient scales with length as  $D \sim 1/N$ , irrespective of  $\theta$ . The relaxation time along the junction scales as  $\tau \sim N^3$  for  $\theta < 135^\circ$ . Reptation along the line of intersection of the two surfaces is also observed for  $\theta \leq 90^\circ$ . Our prediction on linearization of polymer chains is in agreement with experimental observation of DNA stretching on a lipid membrane supported on a grooved substrate.<sup>11</sup>

The present molecular dynamics study revealed the mechanism that governs localization and stretching of polymers on grooved substrates. Stretching of a polymer chain on a substrate with a curved region is very significant, as it has many advantages over the traditional methods. It avoids any flow, and avoids the difficulties of inserting macromolecules inside micro fluidic channels in order to stretch it. Stretched molecules on the substrate could be exposed to a larger surrounding. Thus, the present work has important implications in single molecule characterization, micro/nanofluidic device design, and biotechnological applications.

#### ACKNOWLEDGMENTS

This work is supported by the Department of Science and Technology (DST), Government of India. The computational resources are provided by the Centre for Development and Advance Computing (CDAC) Pune, India, and the HPC cluster of the Computer Center (CC), Indian Institute of Technology Kanpur. T.K.P. acknowledges the Council of Scientific and Industrial Research (CSIR), Government of India, for a senior research fellowship (SRF).

- <sup>1</sup>M. Muthukumar, *Annu. Rev. Biophys. Biomol. Struct.* **36**, 435 (2007); J. Mathe, A. Aksimentiev, D. R. Nelson, K. Schulten, and A. Meller, *Proc. Natl. Acad. Sci. U.S.A.* **102**, 12377 (2005); J. D. Coninck and T. D. Blake, *Annu. Rev. Mater. Res.* **38**, 1 (2008); K. D. Dorfman, S. B. King, D. W. Olson, J. D. P. Thomas, and D. R. Tree, *Chem. Rev.* **113**, 2584 (2013); L. D. Site, C. F. Abrams, A. Alavi, and K. Kremer, *Phys. Rev. Lett.* **89**, 156103 (2002); S. C. Bae and S. Granick, *Annu. Rev. Phys. Chem.* **58**, 353 (2007); G. W. Slater, C. Holm, M. V. Chubynsky, H. W. d. Haan, A. Dube, K. Grass, O. A. Hickey, C. Kingsburry, D. Sean, T. N. Shendruk, and L. Zha, *Electrophoresis* **30**, 792 (2009); F. Persson and J. O. Tegenfeldt, *Chem. Soc. Rev.* **39**, 985 (2010); K. Binder, A. Milchev, and J. Baschnagel, *Annu. Rev. Mater. Sci.* **26**, 107 (1996).
- <sup>2</sup>A. Milchev, *J. Phys.: Condens. Matter* **23**, 103101 (2011).
- <sup>3</sup>M. Rubinstein and R. H. Colby, *Polymer Physics* (Oxford University Press, Oxford, 2003).
- <sup>4</sup>B. Li, X. Fang, H. Luo, Y.-S. Seo, E. Petersen, Y. Ji, M. Rafailovich, J. Sokolov, D. Gersappe, and B. Chu, *Anal. Chem.* **78**(4743), 4743 (2006).
- <sup>5</sup>J. Han, S. W. Turner, and H. G. Craighead, *Phys. Rev. Lett.* **83**(8), 1688 (1999).
- <sup>6</sup>Z. Wang, Z. Jia, and X. He, *Soft Matter* **9**, 11107 (2013).
- <sup>7</sup>A. Ghosh, T. K. Patra, R. Kant, R. K. Singh, J. K. Singh, and S. Bhattacharya, *App. Phys. Lett.* **98**, 164102 (2011).
- <sup>8</sup>A. Milchev, W. Paul, and K. Binder, *Macromol. Theory Simul.* **3**, 305 (1994); J. Han and H. G. Craighead, *Science* **288**, 1026 (2000); N. Pernodet, V. Samuilov, K. Shin, J. Sokolov, M. H. Rafailovich, D. Gersappe, and B. Chu, *Phys. Rev. Lett.* **85**(26), 5651 (2000); N. Hoda and S. Kumar, *J. Chem. Phys.* **128**, 164907 (2008); A. Milchev and K. Binder, *Macromolecules* **29**, 343 (1996).
- <sup>9</sup>T. G. Desai, P. Koblinski, S. K. Kumar, and S. Granick, *Phys. Rev. Lett.* **98**, 218301 (2007).
- <sup>10</sup>B. Maier and J. O. Radler, *Phys. Rev. Lett.* **82**(9), 1911 (1999).
- <sup>11</sup>M. B. Hochrein, J. A. Leierseder, L. Golubovic, and J. O. Radler, *Phys. Rev. Lett.* **96**, 038103 (2006).
- <sup>12</sup>B. Maier and J. O. Radler, *Macromolecules* **33**, 7185 (2000); C.-M. Chang, Y.-G. Lau, J.-C. Tsai, and W.-T. Juan, *Euro. Phys. Lett.* **99**, 48008 (2012).
- <sup>13</sup>Q.-L. Cao, W.-L. Wang, Y. D. Li, and C. S. Liu, *J. Chem. Phys.* **134**, 044508 (2011); S. F. Hsieh and H. H. Wei, *Phys. Rev. E* **79**, 021901 (2009).
- <sup>14</sup>Y. Kim, K. S. Kim, K. L. Kounovsky, R. Chang, G. Y. Jung, J. J. de Pablo, K. Jo, and D. C. Schwartz, *Lab Chip* **11**, 1721 (2011).
- <sup>15</sup>Y. Wang, D. R. Tree, and K. D. Dorfman, *Macromolecules* **44**, 6594 (2011); W. Reisner, K. J. Morton, R. Riehn, Y. M. Wang, Z. Yu, M. Rosen, J. C. Sturm, S. Y. Chou, E. Frey, and R. H. Austin, *Phys. Rev. Lett.* **94**, 196101 (2005); J. W. Yeh, A. Taloni, Y.-L. Chen, and C.-F. Chou, *Nano Lett.* **12**, 1597 (2012); A. Balducci, C.-C. Hsieh, and P. S. Doyle, *Phys. Rev. Lett.* **99**, 238102 (2007); N. Douville, D. Huh, and S. Takayama, *Anal. Bioanal. Chem.* **391**, 2395 (2008); Y. L. Chen, M. D. Graham, J. J. de Pablo, G. C. Randall, M. Gupta, and P. S. Doyle, *Phys. Rev. E* **70**, 060901(R) (2004); Y. Jung, S. Jun, and B.-Y. Ha, *ibid.* **79**, 061912 (2009); J. Tang, S. L. Levy, D. W. Trahan, J. J. Jones, H. G. Craighead, and P. S. Doyle, *Macromolecules* **43**, 7368 (2010); J. Wang and H. Gao, *J. Mech. Behav. Biomed. Mater* **4**, 174 (2011); Y.-J. Sheng and M.-C. Wang, *J. Chem. Phys.* **114**, 4724 (2001).
- <sup>16</sup>J. Kim, C. Jeon, H. Jeong, Y. Jung, and B.-Y. Ha, *Soft Matter* **9**, 6142 (2013).
- <sup>17</sup>P. G. de Gennes, *Scaling Concepts in Polymer Physics* (Cornell University Press, Ithaca, 1979).
- <sup>18</sup>D. Mukherji, G. Bartels, and M. H. Muser, *Phys. Rev. Lett.* **100**, 068301 (2008).
- <sup>19</sup>P. Cifra, *J. Chem. Phys.* **131**, 224903 (2009).
- <sup>20</sup>S. A. Sukhishvili, Y. Chen, J. D. Müller, E. Gratton, K. S. Schweizer, and S. Granick, *Nature (London)* **406**, 146 (2000).
- <sup>21</sup>H.-J. Qian, L.-J. Chen, Z.-Y. Lu, and Z.-S. Li, *Phys. Rev. Lett.* **99**, 068301 (2007); N. Hoda and S. Kumar, *Phys. Rev. E* **79**, 020801(R) (2009); A. L. Ponomarev, T. D. Sewell, and C. J. Durning, *J. Polym. Sci. B: Polym. Phys.* **38**, 1146 (2000).
- <sup>22</sup>T. G. Desai, P. Koblinski, and S. K. Kumar, *J. Chem. Phys.* **128**, 044903 (2008).
- <sup>23</sup>S. A. Sukhishvili, Y. Chen, J. D. Muller, E. Gratton, K. S. Schweizer, and S. Granick, *Macromolecules* **35**, 1776 (2002).
- <sup>24</sup>T. G. Desai, P. Koblinski, S. K. Kumara, and S. Granick, *J. Chem. Phys.* **124**, 084904 (2006); R. Azuma and H. Takayama, *ibid.* **111**, 8666 (1999).

- <sup>25</sup>P. E. Rouse, *J. Chem. Phys.* **21**, 1272 (1953).
- <sup>26</sup>W. Paul, K. Binder, D. W. Heermann, and K. Kremer, *J. Chem. Phys.* **95**, 7726 (1991).
- <sup>27</sup>A. D. Virgiliis, L. Kuban, J. Paturej, and D. Mukherji, *J. Chem. Phys.* **137**, 114902 (2012).
- <sup>28</sup>D. Mukherji and M. H. Muser, *Phys. Rev. E* **74**, 010601(R) (2006).
- <sup>29</sup>G. S. Grest and K. Kremer, *Phys. Rev. A* **33**, 3628 (1986); K. Kremer and G. S. Grest, *J. Chem. Phys.* **92**, 5057 (1990).
- <sup>30</sup>D. Frenkel and B. Smit, *Understanding Molecular Simulation* (Academic Press, 1996).
- <sup>31</sup>S. J. Plimpton, *J. Comput. Phys.* **117**, 1 (1995).
- <sup>32</sup>T. K. Patra, A. Hens, and J. K. Singh, *J. Chem. Phys.* **137**, 084701 (2012).
- <sup>33</sup>K. Avramova and A. Milchev, *J. Chem. Phys.* **124**, 024909 (2006).